Numerical study of the influence of wall compliance on the hemodynamics in a patient-specific arteriovenous fistula

I. DECORATO[a], Z. KHARBOUTLY[a], C. LEGALLAIS[a] and A.V. SALSAC[a]

[a] *Laboratoire Biomécanique et Bioingénierie (UMR CNRS 6600), Université de Technologie de Compiègne, BP 20529, 60205 Compiègne, FRANCE*

Résumé :

Une fistule artério-veineuse (FAV) est une connexion vasculaire entre une artère et une veine. Elle est créée par voie chirurgicale chez les insuffisants rénaux chroniques arrivés au stade terminal afin d'obtenir un accès sanguin suffisant (supérieur à 300 *ml.min*$^{-1}$ *dans la veine) pour l'hémodialyse. Notre objectif est d'étudier l'hémodynamique locale dans une fistule patient-spécifique en simulant numériquement les interactions fluide-structure. On considère le cas d'une FAV latéro-terminale réalisée entre l'extrémité de la veine céphalique et l'artère brachiale. La géométrie de la lumière des vaisseaux est obtenue par reconstruction volumique à partir d'images d'angiographie CT-scan. La paroi des vaisseaux est modélisée par une monocouche d'éléments de coque d'épaisseur constante, l'épaisseur de la paroi vasculaire ne pouvant être obtenue par les images médicales. Les équations qui gouvernent l'écoulement sanguin et le mouvement de la paroi sont résolues en couplant implicitement ANSYS-CFX et ANSYS-Mechanical (ANSYS, Inc.). Pour les conditions aux limites, nous imposons un profil de vitesse instationnaire physiologique en entrée et une valeur de résistance en sortie. Le comportement hyper-élastique de la paroi vasculaire est modélisé par la loi constitutive de Yeoh du 3*ème *ordre. L'évolution spatio-temporelle de la contrainte pariétale (WSS) et de son index d'oscillation (OSI) est étudiée et comparée aux résultats obtenus dans le cas de parois rigides pour quantifier l'effet de la compliance des vaisseaux. Les résultats confirment que les FAV sont soumises à une hémodynamique complexe. Des zones de recirculation sont présentes en particulier dans la veine. Les régions de WSS et OSI non physiologiques correspondent aux régions, qui sont cliniquement les plus sujettes aux lésions de la paroi du vaisseau. Les simulations avec parois rigides surestiment le WSS de 10-13%, l'OSI de 18% et les gradients temporels du WSS à l'anastomose de 10%.*

Abstract:

*An arteriovenous fistula (AVF) is a surgical vessel connection between an artery and a vein. It is created in end stage renal disease to provide adequate blood access (*300-500 *ml.min*$^{-1}$ *in the vein) for hemodialysis. In the present study, the local hemodynamics is investigated in a patient-specific AVF using a computational fluid structure interaction (FSI) simulation. We focus on an end-to-side fistula between the end of the cephalic vein and the brachial artery. The geometry of the vessel lumen is obtained by volume reconstruction from CT-scan angiography. The vessel wall is modelled as a monolayer of shell elements of uniform thickness, since the actual wall thickness cannot be obtained from medical images. The fluid and solid governing equations are solved coupling implicitly ANSYS-CFX and ANSYS-Mechanical (ANSYS, Inc.). A physiological time-dependent velocity inlet profile and constant values of outlet resistance are imposed as boundary conditions for the blood flow. The 3*rd *order Yeoh constitutive law is used to model the hyperelastic behaviour of the vessel wall. We quantify the time- and space-evolution of wall shear stress (WSS) and oscillatory shear index (OSI) and compare the results with rigid wall simulations to quantify the effect of the vessel wall compliance. The results confirm that AVFs are subjected to complex hemodynamics, the vein being in particular dominated by recirculating flows. Regions of pathological WSS and OSI match regions that are mainly prone to wall lesions in clinical practice. Rigid wall simulations overestimate the WSS by 10-13%, the OSI by about 18% and the WSS temporal gradients at the anastomosis by 10%.*

Keywords: arteriovenous fistula, fluid-structure interaction, hemodynamics, wall shear stress, oscillatory shear index

1 Introduction

Most patients with end stage renal disease require hemodialysis. This treatment necessitates a permanent vascular access easily available and able to provide a blood flow higher than 300 $ml.min^{-1}$. An arteriovenous fistula (AVF) is a surgically-created connection between an artery and a vein. Subjected to arterial pressure, the vein gets arterialized, a process that takes about three months. When the fistula reaches its mature state, it acts as a low resistance, high compliance pathway between the high pressure arterial system and the low pressure venous system[1]. The lifespan of an AVF is limited from a few days to about 10 years, the failure being due to insufficient or excessive blood flow inside the cephalic vein. If the reason for failure remains an open question, one of the principal hypotheses is that the altered hemodynamics and the non-physiological flow rate in the vein play an important role in the evolution and long-term efficiency of the AVF. A direct correlation between AVF failure and hemodynamic parameters has been shown[2]. The investigation of hemodynamics cannot be easily performed *in vivo*: Echo Doppler measurements can provide the averaged velocity inside vessels but neither local velocity profiles nor parameters such as the wall shear stress (WSS). The hemodynamics inside the AVF has previously been investigated using computational fluid dynamics simulations[3-4]. These studies have shown a correlation between hemodynamic parameters and local vessel damages, but they neglected both the compliance of the vessel wall and the presence of resistive vessels downstream of the AVF. The aim of the present study is to investigate the fluid structure interaction (FSI) numerically in an AVF, and draw up an accurate map of hemodynamic parameters. The results are compared to rigid wall simulations to quantify the impact of the wall compliance.

2 Methods

Our purpose is to define a patient-specific FSI model that takes into account not only the vessel wall compliance, but also the presence of resistive vessels downstream of the AVF. We analyze a patient's end-to-side brachio-cephalic fistula at the elbow region. It was created by connecting the end of the cephalic vein to the brachial artery.

2.1 Geometry and mesh

The geometry consists of the AVF lumen reconstructed from CT-scan angiography medical images[3]. As region of interest we consider a portion of the AVF consisting of the anastomosis and part of the proximal brachial artery, distal brachial artery and cephalic vein (figure 1a). The lengths of the vessel portions are 4 cm, 3.5 cm, 2 cm respectively from the anastomosis. Cylinders (10 local diameter in length) are extruded at the three extremities in order to impose the boundary conditions away from the region of interest. The vessel wall is modelled as a monolayer of shell elements. The wall thickness is set to be equal to 0.1 times the diameter of the brachial artery, since the actual value cannot be obtained from medical images. The mesh consists of 25×10^3 shell elements for the vessel wall and 231×10^3 elements for the vessel lumen.

2.2 Numerical Model

The fluid structure interactions are simulated coupling ANSYS-CFX and ANSYS-Mechanical (ANSYS, Inc.) implicitly. A convergence study has been done in order to tune the coupling parameters and time-step and to guarantee numerical stability.

2.3 Mechanical and rheological properties

The vessel wall is modelled as homogeneous, isotropic and hyperelastic. Both the artery and the vein are assumed to follow the 3rd-order Yeoh law[5] and to have the same mechanical properties. The law constants are chosen, so that the diameter of the mid-brachial artery varies by 10% over one cardiac cycle.

Blood is modelled as isotropic and homogeneous with a density of 1050 $kg.m^{-3}$. We used both Newtonian and non-Newtonian constitutive laws to model blood in order to quantify possible non-Newtonian effects. For the Newtonian model, the viscosity is considered equal to 4×10^{-3} Pa.s. For the non-Newtonian model, the apparent viscosity μ follows Casson model:

$$\sqrt{\mu} = \sqrt{\frac{\tau_0}{\dot{\gamma}}} + \sqrt{k} \tag{1}$$

where τ_0 represents the yield stress, $\dot{\boldsymbol{\gamma}}$ the shear rate and k the consistency. The model parameters are chosen following experimental data obtained at low shear rates[6]: $\tau_0 = 4\times10^{-3}$ Pa, $k = 3.02\times10^{-3}$ Pa.s.

2.4 Boundary conditions

The time-dependent evolution of the mean velocity U has been measured by echo-Doppler on the patient on the same day as the CT-scan. It is shown in figure 1b as a function of the time non-dimensionalized by the cardiac period T. The velocity U is imposed at the inlet of the tube added to the proximal brachial artery (figure 1a). The peak Reynolds number is 800, mean Reynolds number 650 and Womersley number 4.

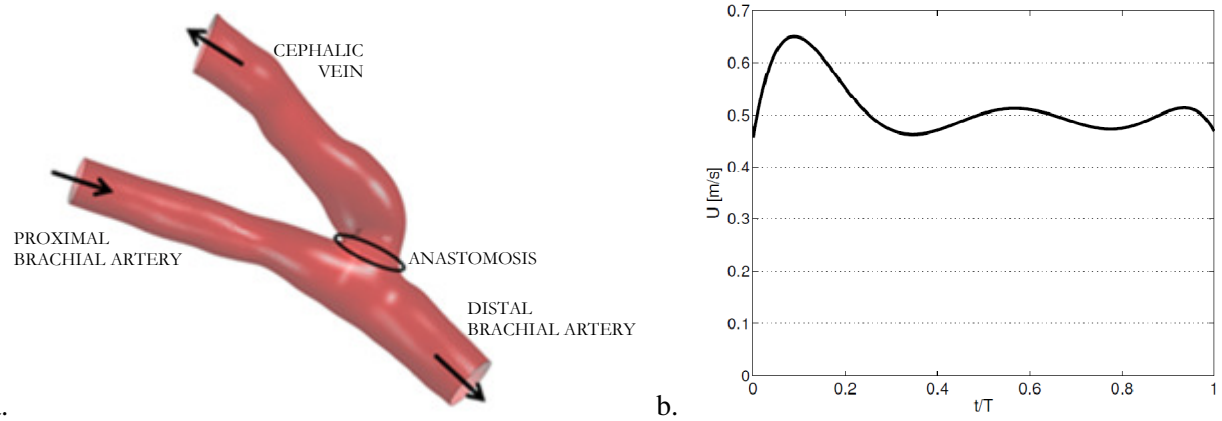

FIG.1 – a. Geometry of the region of interest. b. Time-dependent evolution of the mean velocity profile U.

At the outlets of the tubes added to the brachial vein and distal brachial artery (figure 1a), we impose purely resistive boundary conditions. The value of the distal brachial artery resistance is set to be 5.38×10^{-5} $m^{-1}.s^{-1}$[7]. As no clinical data could be found for the venous resistance, it was tuned to obtain a minimum flow rate of 300 $ml.min^{-1}$ in the cephalic vein, which is the lowest value for a mature functional AVF.

2.5 Hemodynamic parameters

We call wall shear stress (WSS) the modulus of the two-component vector:

$$\boldsymbol{\tau}_{\mathbf{w}} = \mu \frac{\partial \mathbf{v}}{\partial \mathbf{n}}, \tag{2}$$

where $\mathbf{v}$ is the velocity vector and $\mathbf{n}$ the unit vector normal to the vessel wall. In an healthy brachial artery, the WSS is 1-2 Pa[2], which we will call the healthy physiological range. The spatial and temporal gradients of WSS ($WSSG_{sp}$, $WSSG_t$) are defined as:

$$WSSG_{sp} = \sqrt{\left(\frac{\partial WSS}{\partial x}\right)^2 + \left(\frac{\partial WSS}{\partial y}\right)^2 + \left(\frac{\partial WSS}{\partial z}\right)^2}; \tag{3}$$

$$WSSG_t = \frac{\partial WSS}{\partial t}. \tag{4}$$

The oscillatory shear index (OSI) is defined by:

$$OSI = 0.5\left(1 - \frac{\left|\int_0^T WSS\, dt\right|}{\int_0^T |WSS|\, dt}\right). \tag{5}$$

By definition, the OSI index varies between 0 and 0.5. It takes into account the oscillations in the flow direction: the larger the index, the more important the wall shear oscillations.

3 Results and discussion

3.1 Hemodynamics

The analysis of the velocity profiles along the AVF shows a time-varying velocity profile following Womersley solution at the inlet of the region of interest in the proximal brachial artery. A peak velocity equal to 1.1 m.s^{-1} is observed at the region of moderate lumen reduction (location A, figure 2a). Downstream of the anastomosis, secondary flows are observed. The highest vorticity is observed in the cephalic vein.

Upstream of the anastomosis the shear rate is everywhere larger than 300 s^{-1}. Blood therefore behaves like a Newtonian fluid: modelling blood with the Casson model provides the same results in the proximal brachial artery as with the Newtonian model. On the contrary, we observe shear rates smaller than 300 s^{-1} downstream of the anastomosis, especially inside the cephalic vein, where they can be lower than 100 s^{-1}. For such small values of shear rates, the non-Newtonian behaviour of blood can no longer be neglected. Modelling blood as Newtonian results in WSS values overestimated by 13-17% inside the vein. Since the vein hemodynamics plays an important role in the long-term efficiency of the AVF, all the results presented hereafter are obtained with the Casson model: modelling the non-Newtonian blood behaviour is needed to ensure a correct map of the hemodynamic parameters everywhere in the AVF.

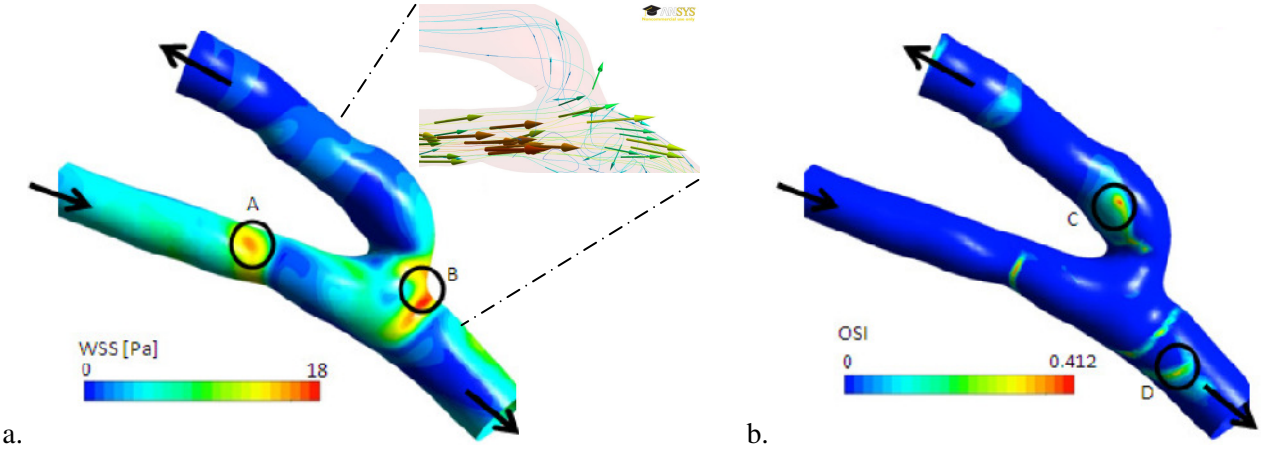

FIG. 2 - Spatial distributions of WSS at peak systole (a) and OSI (b). The inserted figure in (a) shows the velocity vectors in the region of the anastomosis. The vector amplitude represents the velocity magnitude.

The spatial distributions of WSS at the peak systole and OSI are plotted in figure 2. In general, the WSS remains within the healthy physiological WSS range (1-2 Pa)[2] in the proximal brachial artery, except at location A. This region, where the lumen is reduced in cross-section, is characterized by a local WSS about 15 Pa. We observe a peak in the OSI values immediately downstream of the lumen reduction: it corresponds to the existence of recirculating flows. This hemodynamic condition may cause intimal hyperplasia upstream of the anastomosis. One may wonder if it could then affect the AVF efficiency. The highest wall shear stress is observed at location B, just next to the point of impact of the incoming flow on the anastomosis (see the insert in figure 2a). The WSS at peak systole is about 18. Local vessel damage can be caused by the impact of the flow coming from the proximal brachial artery. Location B is otherwise subjected low values of OSI. Downstream of the anastomosis, large areas with WSS values lower than the physiological range are observed on the wall of the distal brachial artery and cephalic vein. Two zones of very high OSI are observed downstream of the anastomosis: locations C and D. Such regions with an OSI larger than 0.3 are characterized by high flow recirculation and wall shear oscillations. They are therefore subjected to non-physiological oscillations, which may be a factor for atherosclerotic plaque formation[2]. The analysis of the distribution of $WSSG_{sp}$ and $WSSG_t$ shows that both quantities are typically very small, their values being almost nil everywhere along the vasculature. They, however, reach very high values at a few locations associated with the regions of high WSS. Both quantities reach their global maximum at peak systole at the point of flow impact on the anastomosis (location B): $WSSG_{sp}$ = 5979.8 Pa.m^{-1}, $WSSG_t$ =78.4 Pa.s^{-1}. For instance, figure 3 shows the time-evolution of $WSSG_t$ at B as compared to a point along the cephalic vein. If $WSSG_{sp}$ appears to play a role in atherosclerotic plaque formation, this role is not completely understood[8]. It is, however, known that endothelial cell proliferation and intimal hyperplasia are found in locations subjected to $WSSG_t$ of large amplitudes and time-variations. Such results have been demonstrated in the case of the AVF anastomosis by Ohja[9].

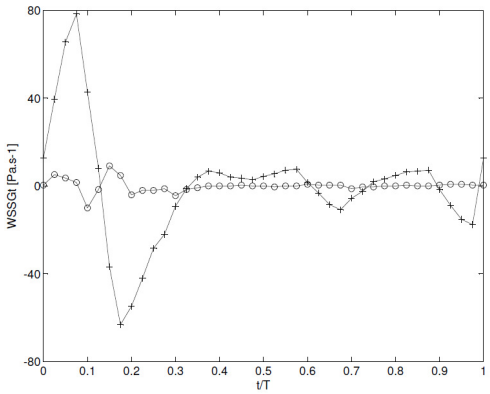

FIG. 3 – Comparison of the temporal variation of $WSSG_t$ at the point of flow impact on the anastomosis (location B) (+) and in the cephalic vein (location C) (○).

3.2 Comparison between rigid wall and compliant wall simulation

Comparing the time variation of WSS in rigid and compliant vessels shows that rigid wall simulations generally overestimate WSS. The WSS are typically 10-13% larger in the rigid case, as shown in table 1. Only at the point of impact and flow separation (location B), the overestimation is 3.1%. The wall compliance tends to reduce the amplitude of the WSS oscillations during the cardiac cycle. This could explain why the OSI is larger in rigid wall simulations (+18.5% at location D and +10% at location C.

If we compare the time variation of $WSSG_t$ in the rigid and compliant wall simulations at location B, the rigid wall model underestimates the oscillation amplitude by 10% but overestimates the frequency of gradient oscillations by 30%. No significant difference has been observed between the rigid and compliant wall on the $WSSG_{sp}$.

TAB. 1 – Comparison of the time-averaged WSS obtained with rigid and compliant wall simulations.

	time-averaged WSS [Pa]		**Δ%**
	rigid wall	**compliant wall**	
proximal brachial artery	2.84	2.51	13.1
cephalic vein	1.31	1.19	10

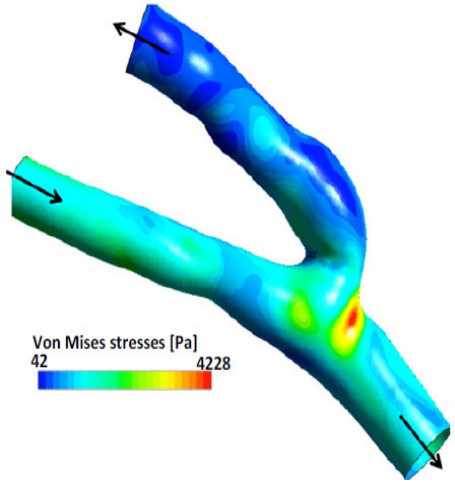

FIG. 4 – Distribution of Von Mises stresses.

3.3 Mechanical constraints

In order to localize the regions of the vessel wall subjected to larger constraints, we represent the distribution of Von Mises stresses in figure 4. The highest stress is observed at the anastomosis. Overall the inner wall constraints are larger on the arterial side than on the venous side. We observe a mean value of 1400 Pa on the

arterial side, whereas it is only 450 Pa on the venous side. One must keep in mind the limitation of the simulation: the results are obtained for vessel mechanical properties identical everywhere in the AVF, which does not mimic the reality. The arterialized vein is likely to be much more rigid than the artery, which will be more elastic. However, the absence of existing data measured on AVF wall tissue so far prevents more realistic simulations to be completed.

4 Conclusions

The originality of this work was to perform an FSI numerical simulation in a patient specific AVF, modelling the vessel wall with a hyperelastic model and blood with a non-Newtonian model. FSI numerical simulations are needed to get realistic results on the hemodynamics and wall dynamics, and therefore on the AVF long-term efficiency.

The results confirm that AVFs are subjected to complex hemodynamics, the vein being in particular dominated by recirculating flows. Regions of pathological WSS and OSI match regions that, in clinical practice, are mainly prone to wall lesions. Rigid wall simulations overestimate the WSS by 10-13%, the OSI by about 18% and the WSS temporal gradients at the anastomosis by 10% .

The case presented herein is specific to one patient; more patients will be studied in the future. The main limitations of the model are the use of purely resistive outlets and the simplification of the geometry away from the AVF (inclusion of straight cylinders). Further improvements will be the implementation of a Windkessel model and the use of the whole fistula geometry.

Acknowledgement

This research is funded by the European Commission, through the MeDDiCA ITN (www.meddica.eu, Marie Curie Actions, grant agreement PITN-GA-2009-238113). The authors gratefully acknowledge Polyclinique St Côme (Compiègne, FRANCE) for the medical images and J. Penrose from ANSYS-UK (ANSYS, Inc.) for all his help and advice.

References

[1] Sivanesan S., How T.V., Black R.A., Bakran A., Flow patterns in the radiocephalic arteriovenous fistula: an in vitro study. *J Biomech*, **32**, 915-925; 1999.

[2] Van Tricht I., De Wachter D., Tordoir J., Verdonck M., Hemodynamics and complications encountered with arteriovenous fistulas and grafts as vascular access for hemodyalisis: a review. *Ann Biomed Eng*, **33**, 1142-1157; 2005.

[3] Kharboutly Z., Fenech M., Treutenaere J.M., Claude I. and Legallais C., Hemodynamics and vascular alterations in an established arteriovenous fistula. *Med Eng Phys*, **29**, 999-1007; 2007.

[4] Ene-Iordache B., Mosconi L., Remuzzi G. and Remuzzi A., Computational fluid dynamics of a vascular access case for hemodialysis. *J Biomech Eng*, **123**, 284-292; 2001.

[5] Yeoh O.H., Some forms of the strein energy function for rubber. *Rubber Chemistry and Technology*, **66**, 754-771; 1993.

[6] Merril E.W. and Pelletier G.A., Viscosity of human blood: transition from Newtonian to non-Newtonian. *J Appl Physiol*, **23**, 179-182; 1967.

[7] Westerhof B.E., Guelen I., Stok W.J., Wesseling K.H., Spaan J.A., Westerhof N., Bos W.J. and Stergiopulos N., Arterial pressure transfer characteristics: effects on travel time. *Am J Physiol Heart Circul Physiol*, **292**, H800-807; 2007.

[8] White C.R, Haidekker M., Bao X. and Frangos J.A., Temporal gradient in shear, but not spatial gradients, stimulate endothelial cell proliferation. *Circulation*, **103**, 2508-2513; 2001.

[9] Ojha M., Wall shear stress temporal gradient and anastomotic intimal hyperplasia. *Circ Res*, **74**, 1227-1231; 1994.